A Highly Sensitive Plasmonic DNA Assay Based on Triangular Silver Nanoprism Etching

Xinjian Yang, Yuebo Yu, and Zhiqiang Gao*

Department of Chemistry, National University of Singapore, Singapore 117543

ABSTRACT Specific nucleic acid detection by using simple and low-cost assays is important in clinical diagnostics, mutation detection, and biodefense applications. Most current methods for the quantification of low concentrations of DNA require costly and sophisticated instruments. Here, we have developed a facile DNA detection platform based on a plasmonic triangular silver nanoprism etching process, in which the shape and size of the nanoprisms were altered accompanied by a substantial surface plasmon resonance shift. Through the combination of enzyme-linked hybridization chain reaction amplification and inherent sensitivity of plasmonic silver nanoprims, this assay could detect as low as 6.0 fM target DNA. Considering the high sensitivity and selectivity of this plasmonic DNA assay, it is expected to be of great interest in clinical diagnostics.

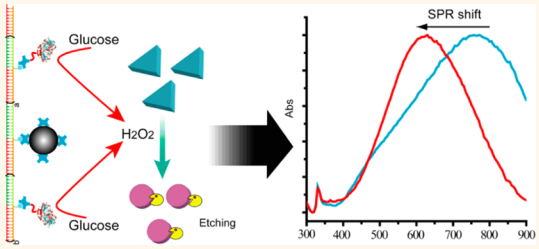

KEYWORDS: plasmonic biosensor · DNA assay · silver nanoprism · etching · HCR · signal amplification

A large number of genetic diseases, such as cancer and mitochondrial diseases, have been revealed to be associated with single-nucleotide polymorphisms (SNPs).[1] Therefore, the ability to detect ultralow concentrations of specific nucleic acid sequences by using simple and low-cost assays is important in clinical diagnostics, mutation detection, and biodefense applications.[2−5] In the past decade, nuclease-based amplification methods such as polymerase chain reaction, ligase chain reaction, and rolling circle amplification have been extensively employed to improve the sensitivity and lower the detection limit.[6−10] Although promising, most of these methods are limited by complex sequence design and sample preparation protocols. Recently, great attention has been focused on signal amplification without the use of nucleases. The rapid emerging research field of strand displacement-based isothermal amplification provides exciting possibilities for advanced development of new analytical tools and instrumentation for bioanalytical applications.[11,12] In particular, the hybridization chain reaction (HCR) is a very useful process, during which a long, linear, double-stranded DNA (ds-DNA) molecule with repeated units is formed through programmed self-assembling triggered by an initiator DNA.[13−18]

Nanomaterial-based technologies provide an exciting avenue that could significantly lower the detection limit of specific analytes. For instance, noble metal nanomaterials that exhibit ultrahigh extinction coefficients of the surface plasmon resonance (SPR) absorption offer an excellent opportunity to construct devices and assays with unparalleled functionalities for highly sensitive target analysis.[19−24] The SPR responses of noble metal nanomaterials are sensitive and strongly affected by structural parameters such as size, shape, interparticle spacing, and the surrounding dielectric environment,[25] making them the basis for biological labeling, sensing, and detection. Among these nanomaterials, silver-based nanomaterials have attracted intensive attention due to their strong shape-dependent optical properties. Compared with gold nanomaterials, the structures and plasmonic properties of silver nanomaterials are subject to changes when exposed to some disturbances.[26,27] Meanwhile, silver nanomaterials produce a much stronger and sharper plasmon resonance.[28−30] Particularly,

* Address correspondence to chmgaoz@nus.edu.sg.

Received for review February 13, 2014 and accepted April 21, 2014.

Published online April 25, 2014
10.1021/nn5008786

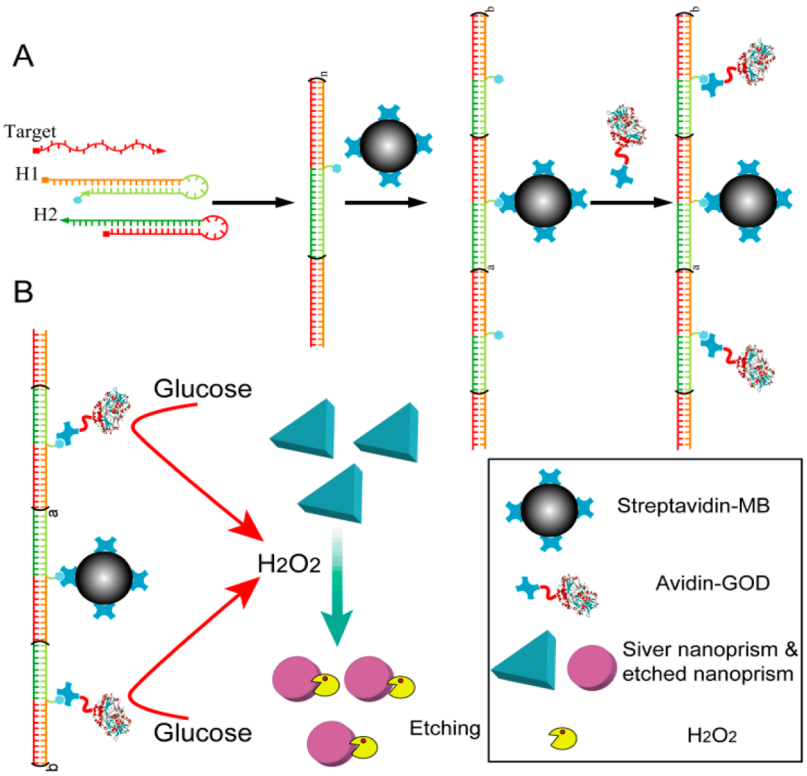

Figure 1. (A) Construction of HCR-based specific DNA detection platform. (B) The sensing mechanism is based on the etching process of triangular silver nanoprisms.

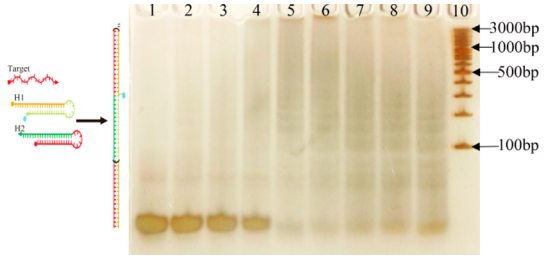

Figure 2. Native polyacrylamide (8%) gel electrophoresis. A concentration of 2.5 μM was used for both H_1 and H_2. The concentrations of the target DNA used from lane 1 to 9 were 0, 0.0625, 0.125, 0.25, 0.5, 0.75, 1.25, 1.875, and 2.5 μM, respectively. The gel was run at 150 V for 60 min in TA buffer.

triangular silver nanoprisms with three-dimensional nanostructures exhibit exquisite features in the localized SPR (LSPR) owing to an extreme degree of anisotropy in their structures.[31] Silver nanomaterials in principle promise a wider range of potential applications, including not only chemical and biological sensing but also imaging and catalysis.[32−37] Therefore, silver nanomaterials are outstanding building blocks for the construction of bioassays when their SPR shifts in response to a biorecognition event. In this report, we demonstrated that plasmonic triangular silver nanoprisms can be applied for highly sensitive DNA detection, where the properties of the plasmonic silver nanoprisms are essential for their efficacy and performance.

RESULTS AND DISCUSSION

Figure 1 schematically depicts the working principle of the assay, which combines the nuclease-free signal amplification and inherent sensitivity of plasmonic silver nanoprisms. Two hairpin DNA strands—biotinylated H_1 and H_2 with one overhang, respectively—were introduced into the system. H_1 can be opened by target DNA strand displacement, and H_2 contains a blocked target DNA sequence that can only be opened triggered by the released single strand in H_1. These two hairpin DNA strands are stable and would not open or hybridize with each other in the absence of the target DNA. In the presence of the target DNA, a cascade of hybridization events is triggered by the target DNA, forming a nicked linear, long ds-DNA with numerous repeat units. Since H_1 is modified with biotin, we can use streptavidin-coated magnetic beads to separate the nicked linear, long ds-DNA from the original hybridization solution and apply avidin-tagged glucose oxidase (avidin-GOD) to interact with the rest of the biotin sites in the linear structure. Therefore, the enzyme amplification and HCR are coupled into one system to achieve a better sensing performance. In the presence of glucose, molecular oxygen is enzymatically reduced to H_2O_2. In turn, H_2O_2 acts as an oxidant to etch the triangular silver nanoprisms into smaller spherical silver nanoparticles accompanied by a substantial blue shift of the SPR peak.

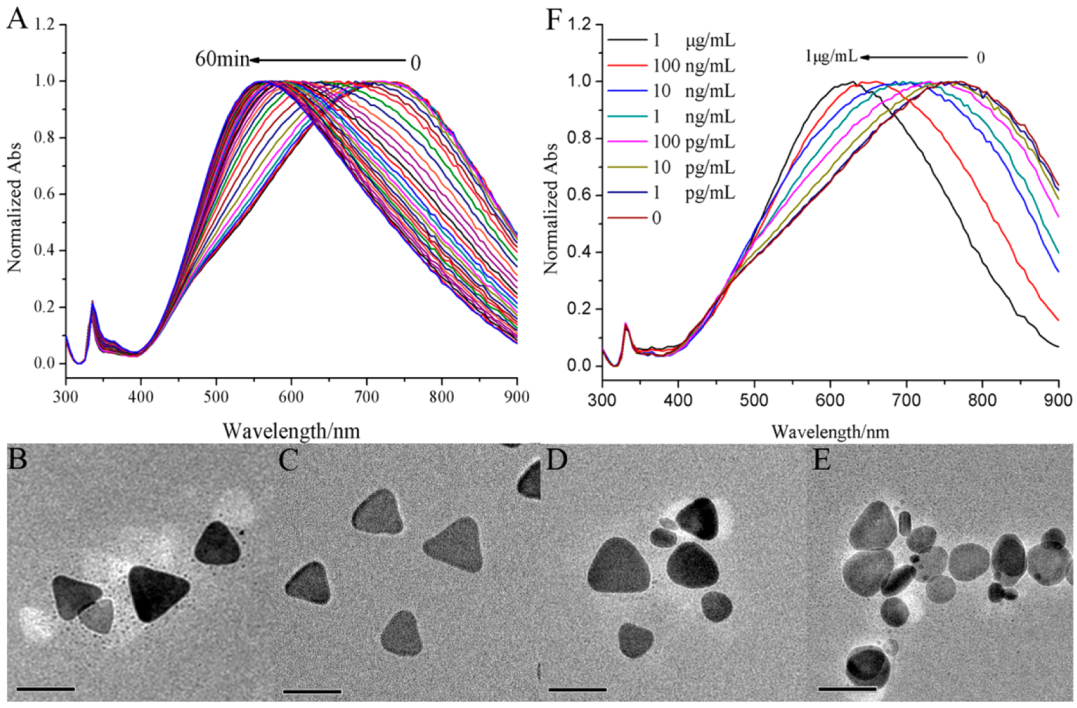

Figure 3. (A) SPR peak shift of triangular silver nanoprisms in the presence of GOD and glucose; (B) TEM images of triangular silver nanoprisms and (C−E) the shape change during the etching process (scale bare is 50 nm); (F) SPR peak of triangular silver nanoprisms in the presence of different concentrations of GOD.

To investigate the formation of the nicked long, linear DNA, gel electrophoresis was first performed to reveal the relationship between the amount of the formed long DNA and the concentration of the target. As shown in Figure 2, in the absence of the target DNA, a well-defined band (lane 1) was observed, which indicates that the two hairpin DNA monomers are stable and the interaction between each other does not happen without the target DNA, while in the presence of the target DNA, a long dispersed band was observed (lanes 2−8). With the increase of the target DNA concentration, more H_1 and H_2 were assembled into a high molecular weight DNA structure. With increasing the amount of the target DNA, more H_1 and H_2 were consumed, reflected by the gradual disappearance of the low H_1+H_2 band at the bottom of the gel. Moreover, a high concentration of the target DNA resulted in the assembly of a broad range of ds-DNA structures of different lengths. This is likely due to the fact that when more target DNA strands are introduced, more assembly sites are formed, leaving less chance for H_1 and H_2 to assemble into longer structure.

Triangular silver nanoprisms with a high extinction coefficient were synthesized according to previous reports.[31] High stability of the silver nanoprisms is the key for the success of the assay. We tested the influence of glucose, DNA, and GOD on the stability of the triangular silver nanoprisms. No noticeable SPR peak shifts were observed upon the addition of these constituents (Figure S1), thus providing the opportunity of using these triangular silver nanoprisms as the indicator in our assay. Previous reports[26] have indicated that the poor chemical and structural stability of the triangular silver nanoprisms are the main issue that prevents their broad use. It is therefore essential to develop strategies to shield them from aggregation and degradation while maintaining their excellent plasmonic properties. Two strategies were attempted to tackle the stability problem. The first strategy was to coat the triangular silver nanoprisms with passivated shells to protect them from etching or other effects. However, this strategy inevitably increased the complexity and decreased their extinction coefficient and consequently the sensitivity of the assay. The second strategy was to separate the target DNA from its original solution after it has interacted with H_1 and H_2. In this connection, magnetic beads were used to separate the target DNA.

Next, we tested the etching process of the triangular silver nanoprisms by hydrogen peroxide. It is well known that H_2O_2 is a powerful oxidizing agent with a strong dependence on the acidity of the solution.[38] Under acidic conditions,

$$H_2O_2 + 2H^+ + 2e^- \rightarrow 2H_2O \quad E^0 = 1.763\ \text{V} \qquad (1)$$

Under alkaline conditions,

$$H_2O_2 + 2e^- \rightarrow 2OH^- \quad E^0 = 0.867\ \text{V} \qquad (2)$$

On the other hand, for the triangular silver nanoprisms, their redox potential is given as follows:

$$Ag^+ + e^- \rightarrow Ag \quad E^0 = 0.7996\ \text{V} \qquad (3)$$

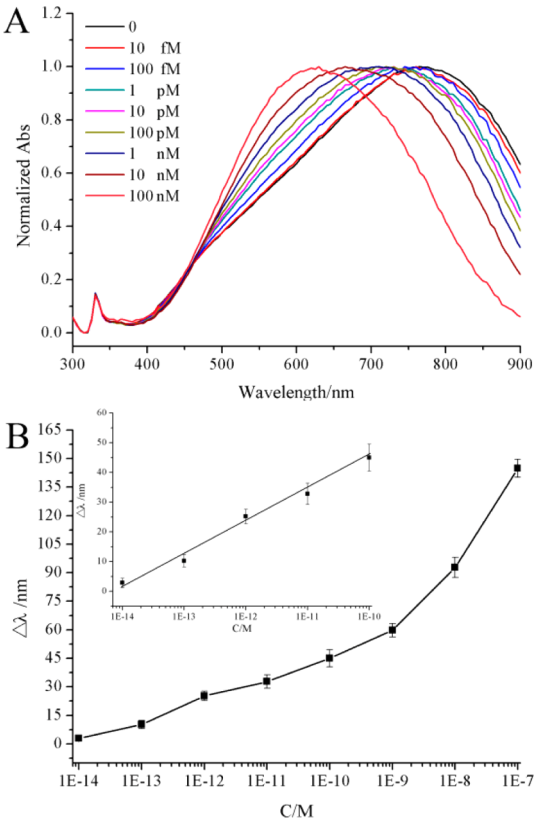

Figure 4. (A) UV−vis spectra of triangular silver nanoprisms in the presence of different concentrations of target DNA; (B) peak shifts of triangular nanoprisms with the concentrations of the target DNA.

It has a standard potential of 1.763 V in acidic solutions and 0.867 V in alkaline solutions, both of which are higher than that of Ag^+/Ag (0.7996 V), thus suggesting that H_2O_2 can be used as an effective etchant to dissolve metallic silver according to the following reactions:

$$\text{glucose} + O_2 \xrightarrow{\text{GOD}} \text{gluconic acid} + H_2O_2 \qquad (4)$$

$$\text{metallic Ag} + H_2O_2 \xrightarrow{\text{etching}} Ag^+ + H_2O \qquad (5)$$

Additionally, the GOD-catalyzed oxidation of glucose produces gluconic acid, which effectively lowers local pH and consequently increases the oxidizing power (potential of H_2O_2/H_2O couple) to speed up the etching process. The etching process was inspected using UV−vis spectrometry. As shown in Figure 3, when GOD and glucose coexisted in the solution, a gradually blue shift of the SPR peak was observed due to the shape change of the triangular silver nanoprisms with the advance of the etching process. TEM images indicated that the morphology of the triangular silver nanoprisms gradually changed from triangular to spherical (Figure 3B−E). It was found that the etching process is GOD concentration dependent. As shown in Figure 3F, higher GOD concentrations produced larger blue shifts of the SPR peak, which paves the way for the development of a highly sensitive DNA assay. Next, we compared the sensitivity of silver nanoprisms with different aspect ratios and other nanostructures (Figure S2). Results showed that with the decrease of aspect ratio, the sensitivity decreased. Meanwhile, other nanostructures such silver-coated gold nanorods or gold nanocages were not suitable for the development of sensitive assays using SPR shift as analytical signal.

To evaluate the sensitivity of this assay for DNA detection, the p53 gene was selected as a model. It has been demonstrated that more than 50% of human solid tumors are connected with mutations in the p53 gene, which is one of the main components of the cell defense system against malignant transformation.[39] As indicated in Figure 1, the linear nicked ds-DNA could be separated from the solution by using magnetic beads. The specific interaction between avidin and biotin is very strong, which guarantees high separation efficiency. However, the excess of biotinylated H_1 strands that do not take part in the assembly process could also be absorbed on the surface of the magnetic beads. Therefore, to eliminate the influence of nonassembled H_1 and H_2, the magnetic beads must possess enough sites to anchor the long, biotin-decorated ds-DNA apart from the nonassembled strands. We tested the SPR peak shift of triangular silver nanoprisms at different H_1 and H_2 concentrations. As shown in Figure S3, when the concentration was 0.5 μM, a maximum peak shift was found. Higher concentrations of H_1 and H_2 decreased the absorption of biotin-decorated, long ds-DNA, while lower concentrations resulted in less biotin-decorated, long ds-DNA formation. Under optimal conditions, we measured the target concentration-dependent SPR peak shift process. As shown in Figure 4, the SPR peak shifted when the concentration of the target was from 10 fM to 100 nM, demonstrating that the etching of the silver nanoprisms by H_2O_2 is strongly dependent on the concentration of the target DNA. A semilogarithmic dependence was obtained between the blue shift of the SPR peak and the concentration of target DNA from 10 fM to 100 pM. The detection limit was calculated to be 6.0 fM based on three times the standard deviation of the control (blank), which was superior to most of the recently reported nuclease-aided amplification assays (Table S1). This high sensitivity was attributed to the combination of enzyme-linked HCR amplification and the use of inherently sensitive triangular silver nanoprisms. These results clearly demonstrated the ability of triangular silver nanoprism etching as a general method for DNA detection with high sensitivity. In addition, we conducted the biosensing by adding serum to the HCR buffer (Figure S5). The result showed that the assay performs well when target DNA is in 10−30% serum, which is very promising for real sample analysis.

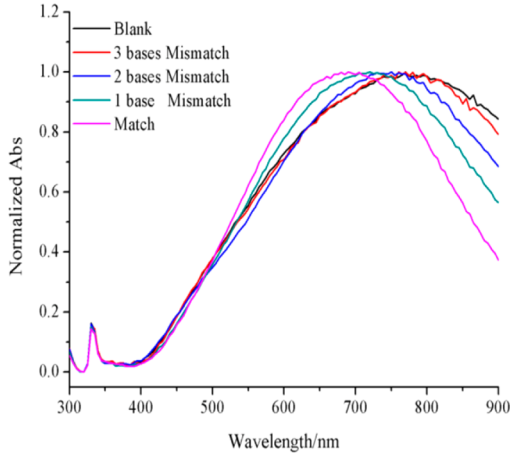

Figure 5. Specificity of the DNA detection. UV−vis spectra of triangular silver nanoprisms in the presence of target DNA (10 nM) with different mismatched bases.

We also investigated the specificity of this triangular silver nanoprism-based DNA assay to differentiate SNPs. Figure 5 shows the UV−vis absorption spectra of the silver nanoprisms in the presence of different DNAs. As shown in Figure 5, the largest SPR peak shift was observed when the target DNA was perfectly matched. However, when the mismatched sequences were introduced in the target DNA, fewer peak shifts occurred. Three-base mismatched DNA induced no peak shift at all. This high specificity is due to the weak strand displacement between target DNA and H_1, which subsequently leads to less long nicked ds-DNA formation (Figure S6). These results indicated that this DNA assay can provide an excellent capability to differentiate between perfectly matched and mismatched DNA targets, demonstrating the excellent selectivity of this assay.

CONCLUSIONS

In summary, we demonstrated a facile DNA detection assay based on a plasmonic triangular silver nanoprism etching process, in which the shape and size of the nanoprisms were altered accompanied by SPR shift. Meanwhile, it combined the enzyme and HCR amplification into one system, which greatly lowered the detection limit. The results indicated that this plasmonic DNA assay can detect as low as 6.0 fM target DNA by simple mixing and magnetic separation. Moreover, this DNA assay also showed high specificity in differentiating SNPs, which makes it a promising platform for biomedical applications. In addition, the assay does not require a sophisticated experimental procedure or equipment. Considering the high sensitivity and selectivity of this plasmonic DNA assay, it is expected to be of great interest in clinical diagnostics. Alternatively, on-chip biosensing devices can also be envisaged by simply changing the avidin-modified magnetic beads with avidin-decorated chips.

EXPERIMENTAL SECTION

Preparation of Triangular Silver Nanoprisms. The triangular silver nanoprisms were synthesized according to a reported procedure.[31] Briefly, $AgNO_3$ (40 μL, 0.1 M), sodium citrate (600 μL, 0.1 M), and H_2O_2 (30 wt %, 112 μL) were mixed with water (final volume: 40 mL) at room temperature and vigorously stirred for 10 min. Then, $NaBH_4$ (100 mM, 400 μL) was rapidly injected into this mixture, and the solution changed gradually from colorless to yellow, red, and blue, indicating the formation of Ag nanoprisms. The resultant triangular nanoprism solution was kept at 4 °C before use.

Native Gel Electrophoresis. H_1 and H_2 (both 50 μM) in buffer (10 mM Tris-Ac, 500 mM NaAc, pH = 6.8) were heated to 95 °C for 5 min and then allowed to cool to room temperature in 2 h before use. Different concentrations of the target DNA were incubated with 2.5 μM H_1 and H_2 at room temperature for 2 h. Then the samples were applied to a polyacrylamide gel (8%, 37.5/1 acrylamide/bis(acrylamide)) to evaluate the formation of the long ds-DNA in 1 × TA buffer at 150 V for 1 h. Gel was stained with silver ions to image the position of DNA. The photographic image was obtained directly with a digital camera.

Assay Procedure. In a typical DNA assay, samples containing target DNA were mixed with H_1 (500 nM) and H_2 (500 nM) in Tris-Ac buffer (100 μL, 10 mM Tris, 500 mM NaAc, 0.05% Triton-100, pH = 6.8) at room temperature for 2 h. Then streptavidin-coated magnetic beads were added into each mixture and kept for 30 min before magnetic separation. The magnetic beads were wash three times using Tris-Ac buffer. Next avidin-GOD (0.8 μL, 5 mg/mL) was mixed with the magnetic beads in Tris-Ac buffer, and the magnetic beads were then separated and washed three times with Tris-Ac buffer. The magnetic beads were mixed with glucose (1.0 mM) in 50 μL of water for 1 h. The supernatant was mixed with the silver triangular nanoprisms (100 μL, the silver naoprisms were centrifuged once before use) for 30 min. Then the absorption was measured on the UV−vis spectrophotometer.

Conflict of Interest: The authors declare no competing financial interest.

Acknowledgment. This work was supported by the A*STAR-ANR program.

Supporting Information Available: Figures S1−S6 and the DNA sequences. This material is available free of charge *via* the Internet at http://pubs.acs.org.

REFERENCES AND NOTES

1. LaFramboise, T. Single Nucleotide Polymorphism Arrays: A Decade of Biological, Computational and Technological Advances. *Nucleic Acids Res.* **2009**, *37*, 4181–4193.
2. Hacia, J. G.; Brody, L. C.; Chee, M. S.; Fodor, S. P. A.; Collins, F. S. Detection of Heterozygous Mutations in BRCA1 Using High Density Oligonucleotide Arrays and Two-Colour Fluorescence Analysis. *Nat. Genet.* **1996**, *14*, 441–447.
3. Collins, F. S.; Hacia, J. G.; Fan, J. B.; Ryder, O.; Jin, L.; Edgemon, K.; Ghandour, G.; Mayer, R. A.; Sun, B.; Hsie, L.; *et al.* Determination of Ancestral Alleles for Human Single-Nucleotide Polymorphisms Using High-Density Oligonucleotide Arrays. *Nat. Genet.* **1999**, *22*, 164–167.
4. Mirkin, C. A.; Rosi, N. L.; Giljohann, D. A.; Thaxton, C. S.; Lytton-Jean, A. K. R.; Han, M. S. Oligonucleotide-Modified Gold Nanoparticles for Intracellular Gene Regulation. *Science* **2006**, *312*, 1027–1030.

5. Lubin, A. A.; Plaxco, K. W. Folding-Based Electrochemical Biosensors: The Case for Responsive Nucleic Acid Architectures. *Acc. Chem. Res.* **2010**, *43*, 496–505.
6. Zhang, H.; Li, F.; Dever, B.; Li, X. F.; Le, X. C. DNA-Mediated Homogeneous Binding Assays for Nucleic Acids and Proteins. *Chem. Rev.* **2013**, *113*, 2812–2841.
7. Piatek, A. S.; Tyagi, S.; Pol, A. C.; Telenti, A.; Miller, L. P.; Kramer, F. R.; Alland, D. Molecular Beacon Sequence Analysis for Detecting Drug Resistance in Mycobacterium Tuberculosis. *Nat. Biotechnol.* **1998**, *16*, 359–363.
8. Abravaya, K.; Carrino, J. J.; Muldoon, S.; Lee, H. H. Detection of Point Mutations with a Modified Ligase Chain Reaction (Gap-LCR). *Nucleic Acids Res.* **1995**, *23*, 675–682.
9. Christian, A. T.; Pattee, M. S.; Attix, C. M.; Reed, B. E.; Sorensen, K. J.; Tucker, J. D. Detection of DNA Point Mutations and mRNA Expression Levels by Rolling Circle Amplification in Individual Cells. *Proc. Natl. Acad. Sci. U.S.A.* **2001**, *98*, 14238–14243.
10. Shen, W.; Deng, H.; Gao, Z. Gold Nanoparticle-Enabled Real-Time Ligation Chain Reaction for Ultrasensitive Detection of DNA. *J. Am. Chem. Soc.* **2012**, *134*, 14678–14681.
11. Chen, X.; Briggs, N.; McLain, J. R.; Ellington, A. D. Stacking Nonenzymatic Circuits for High Signal Gain. *Proc. Natl. Acad. Sci. U.S.A.* **2013**, *110*, 5386–5391.
12. Choi, H. M.; Chang, J. Y.; Trinh le, A.; Padilla, J. E.; Fraser, S. E.; Pierce, N. A. Programmable *in Situ* Amplification for Multiplexed Imaging of mRNA Expression. *Nat. Biotechnol.* **2010**, *28*, 1208–1212.
13. Wang, F.; Elbaz, J.; Orbach, R.; Magen, N.; Willner, I. Amplified Analysis of DNA by the Autonomous Assembly of Polymers Consisting of DNAzyme Wires. *J. Am. Chem. Soc.* **2011**, *133*, 17149–17151.
14. Huang, J.; Wu, Y.; Chen, Y.; Zhu, Z.; Yang, X.; Yang, C. J.; Wang, K.; Tan, W. Pyrene-Excimer Probes Based on the Hybridization Chain Reaction for the Detection of Nucleic Acids in Complex Biological Fluids. *Angew. Chem., Int. Ed.* **2011**, *50*, 401–404.
15. Dirks, R. M.; Pierce, N. A. Triggered Amplification by Hybridization Chain Reaction. *Proc. Natl. Acad. Sci. U.S.A.* **2004**, *101*, 15275–15278.
16. Niu, S.; Jiang, Y.; Zhang, S. Fluorescence Detection for DNA Using Hybridization Chain Reaction with Enzyme-Amplification. *Chem. Commun.* **2010**, *46*, 3089–3091.
17. Zhang, B.; Liu, B.; Tang, D.; Niessner, R.; Chen, G.; Knopp, D. DNA-Based Hybridization Chain Reaction for Amplified Bioelectronic Signal and Ultrasensitive Detection of Proteins. *Anal. Chem.* **2012**, *84*, 5392–5399.
18. Xu, J.; Wu, J.; Zong, C.; Ju, H.; Yan, F. Manganese Porphyrin-dsDNA Complex: A Mimicking Enzyme for Highly Efficient Bioanalysis. *Anal. Chem.* **2013**, *85*, 3374–3379.
19. Hess, O.; Pendry, J. B.; Maier, S. A.; Oulton, R. F.; Hamm, J. M.; Tsakmakidis, K. L. Active Nanoplasmonic Metamaterials. *Nat. Mater.* **2012**, *11*, 573–584.
20. Anker, J. N.; Hall, W. P.; Lyandres, O.; Shah, N. C.; Zhao, J.; Van Duyne, R. P. Biosensing with Plasmonic Nanosensors. *Nat. Mater.* **2008**, *7*, 442–453.
21. He, H.; Xu, X.; Wu, H.; Jin, Y. Enzymatic Plasmonic Engineering of Ag/Au Bimetallic Nanoshells and Their Use for Sensitive Optical Glucose Sensing. *Adv. Mater.* **2012**, *24*, 1736–1740.
22. de la Rica, R.; Stevens, M. M. Plasmonic ELISA for the Ultrasensitive Detection of Disease Biomarkers with the Naked Eye. *Nat. Nanotechnol.* **2012**, *7*, 821–824.
23. Rodríguez-Lorenzo, L.; de la Rica, R.; Álvarez-Puebla, R. A.; Liz-Marzán, L. M.; Stevens, M. M. Plasmonic Nanosensors with Inverse Sensitivity by Means of Enzyme-Guided Crystal Growth. *Nat. Mater.* **2012**, *11*, 604–607.
24. Wu, H. J.; Henzie, J.; Lin, W. C.; Rhodes, C.; Li, Z.; Sartorel, E.; Thorner, J.; Yang, P.; Groves, J. T. Membrane-Protein Binding Measured with Solution-Phase Plasmonic Nanocube Sensors. *Nat. Methods* **2012**, *9*, 1189–1191.
25. Jain, P. K.; Huang, X.; El-Sayed, I. H.; El-Sayed, M. A. Noble Metals on the Nanoscale: Optical and Photothermal Properties and Some Applications in Imaging, Sensing, Biology, and Medicine. *Acc. Chem. Res.* **2008**, *41*, 1578–1586.
26. Gao, C.; Lu, Z.; Liu, Y.; Zhang, Q.; Chi, M.; Cheng, Q.; Yin, Y. Highly Stable Silver Nanoplates for Surface Plasmon Resonance Biosensing. *Angew. Chem., Int. Ed.* **2012**, *51*, 5629–5633.
27. Xia, Y.; Ye, J.; Tan, K.; Wang, J.; Yang, G. Colorimetric Visualization of Glucose at the Submicromole Level in Serum by a Homogenous Silver Nanoprism-Glucose Oxidase System. *Anal. Chem.* **2013**, *85*, 6241–6247.
28. Wiley, B.; Sun, Y.; Mayers, B.; Xia, Y. Shape-Controlled Synthesis of Metal Nanostructures: the Case of Silver. *Chem.—Eur. J.* **2005**, *11*, 454–463.
29. Pastoriza-Santos, I.; Liz-Marzan, L. M. Colloidal Silver Nanoplates. State of the Art and Future Challenges. *J. Mater. Chem.* **2008**, *18*, 1724–1737.
30. Millstone, J. E.; Hurst, S. J.; Metraux, G. S.; Cutler, J. I.; Mirkin, C. A. Colloidal Gold and Silver Triangular Nanoprisms. *Small* **2009**, *5*, 646–664.
31. Zhang, Q.; Li, N.; Goebl, J.; Lu, Z.; Yin, Y. A Systematic Study of the Synthesis of Silver Nanoplates: Is Citrate A "Magic" Reagent? *J. Am. Chem. Soc.* **2011**, *133*, 18931–18939.
32. Cao, Y. C.; Jin, R.; Mirkin, C. A. Nanoparticles with Raman Spectroscopic Fingerprints for DNA and RNA Detection. *Science* **2002**, *297*, 1536–1540.
33. Nie, S.; Emory, S. R. Probing Single Molecules and Single Nanoparticles by Surface-Enhanced Raman Scattering. *Science* **1997**, *275*, 1102–1106.
34. Lee, K. S.; El-Sayed, M. A. Gold and Silver Nanoparticles in Sensing and Imaging: Sensitivity of Plasmon Response to Size, Shape, and Metal Composition. *J. Phys. Chem. B* **2006**, *110*, 19220–19225.
35. Wodka, D.; Bielan′ska, E.; Socha, R. P.; Elz·bieciak-Wodka, M.; Gurgul, J.; Nowak, P.; Warszyn′ski, P.; Kumakiri, I. Photocatalytic Activity of Titanium Dioxide Modified by Silver Nanoparticles. *ACS Appl. Mater. Interfaces* **2010**, *2*, 1945–1953.
36. Christopher, P.; Xin, H.; Linic, S. Visible-Light-Enhanced Catalytic Oxidation Reactions on Plasmonic Silver Nanostructures. *Nat. Chem.* **2011**, *3*, 467–472.
37. Malile, B.; Chen, J. I. Morphology-Based Plasmonic Nanoparticle Sensors: Controlling Etching Kinetics with Target-Responsive Permeability Gate. *J. Am. Chem. Soc.* **2013**, *135*, 16042–16045.
38. Ho, C. M.; Yau, S. K.; Lok, C. N.; So, M. H.; Che, C. M. Oxidative Dissolution of Silver Nanoparticles by Biologically Relevant Oxidants: A Kinetic and Mechanistic Study. *Chem.—Asian J.* **2010**, *5*, 285–293.
39. Gerion, D.; Chen, F. Q.; Kannan, B.; Fu, A. H.; Parak, W. J.; Chen, D. J.; Majumdar, A.; Alivisatos, A. P. Room-Temperature Single-Nucleotide Polymorphism and Multiallele DNA Detection Using Fluorescent Nanocrystals and Microarrays. *Anal. Chem.* **2003**, *75*, 4766–4772.